REVIEW OF THE APS SR RF SYSTEMS

J.J. Song, A. Cours, A. Grelick, K. Harkay, D. Horan, Y.W. Kang, R.L. Kustom, A. Nassiri, G. Pile, and T. L. Smith, Advanced Photon Source, Argonne National Laboratory, 9700 S. Cass Ave., Argonne, Illinois 60439, USA

Abstract

The Advanced Photon Source (APS) is a 7-GeV full energy storage ring (SR) for generating synchrotron radiation with an injector. The storage ring cavities consist of four groups of four single cells powered by up to four 1-MW klystrons for up to 300-mA operation. A review of the operation of the rf system as well as rf-related beam dynamics is presented [1]. This review includes rf power distribution, low-level feedback, control law, beam loading, beam instabilities, higher-order modes, and beam-induced multipactoring.

1 INTRODUCTION

The SR rf system consists of four groups of four single-cell cavities powered by two 1-MW klystrons for nominal operation at 100-mA. Two additional 1-MW transmitters are added to the existing system to support the ultimate design goal of 300 mA at 7 GeV. At least three transmitters are needed for 300-mA operation, affording one hot spare for 300-mA operation. The rf parameters are summarized in Table 1.

Table 1: Storage Ring RF Parameters

Max voltage/cavity	1.00		MV
Shunt resistance	5.60		MW
Max power	89.2		kW
Quality factor (unloaded), Q	4.3		10^3
Beam current	100	300	mA
Voltage	9.5	9.5	MV
Voltage per cavity	593.8	593.8	kV
Power per cavity	31.5	31.5	kW
Total power	503.7	503.7	kW
Beam power per cavity	43.1	129.3	kW
Sum	74.6	160.8	kW
Q (loaded)	21.1	9.9	10^3
Bandwidth (loaded)	8.3	18.4	kHz
Power lost to cavity	8.1	17.3	kW
Source power	1.32	2.85	MW

2 RF OPERATION

2.1 RF Power Distribution

For reliable and continuous operation of the booster synchrotron and the storage ring rf systems, the five rf transmitters can be reconfigured to afford redundancy in operation using WR-2300 waveguide switches. The design of the waveguide switching system for rf power distribution in the APS is shown in Figure 1. The 90˚ quadrature hybrids and 45˚ phase shifters in the WR2300 waveguide are used as the elements for combining and splitting the power [2].

The switching system is equipped with an equipment safety interlock system through an rf power monitoring system. The system is controlled by a programmable logic controller (PLC) unit independent from the main computer control system of the accelerators. The waveguide circuit has been completely installed and has powered the booster and storage ring systems successfully.

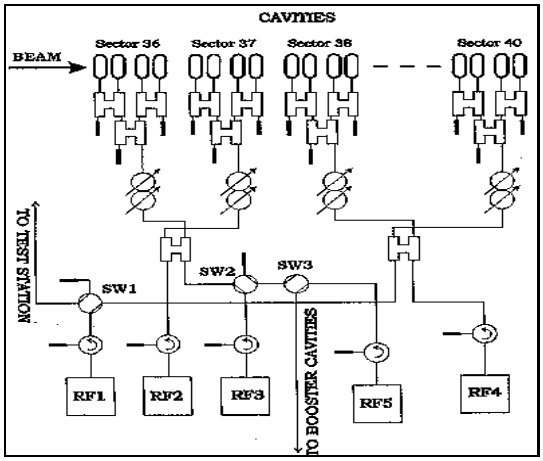

Figure 1: Reconfigurable waveguide switching system.

2.2 Low-Level RF

The low-level rf system for the storage ring klystron consists of two phase loops, one nested within the other. The internal phase loop removes phase jitters in the klystron output caused by high-voltage power supply (HVPS) ripple. The cavity low-level rf system consists of a phase loop around each cavity to maintain proper phase between the forward power and field probe output. Phase errors are adjusted by moving a piston tuner to keep the cavity at resonance. Envelope detectors are used throughout the system to measure rf power and to determine gap voltage.

Phase loop bandwidth tests were performed on the Advanced Photon Source storage ring 352-MHz rf systems, as shown in Figure 2 [3]. An electronic phase shifter was used to inject approximately 14 degrees of stimulated phase shift into the low-level rf system, which produced measurable response voltage in the feedback loops without upsetting normal rf system operation. With the PID (proportional-integral-differential) amplifier settings at the values used during accelerator operation, the measurement data revealed that the 3-dB response for the cavity sum and klystron power-phase loops was approximately 7 kHz and 45 kHz, respectively, with the cavities being the primary bandwidth-limiting factor in the cavity-sum loop.

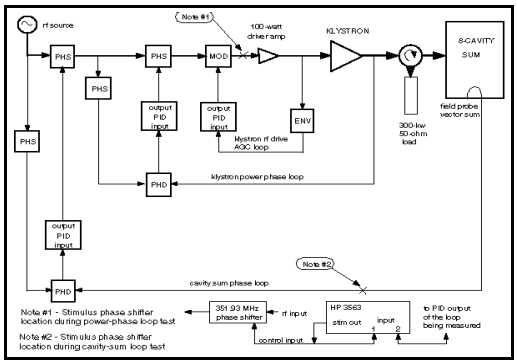

Figure 2: Setup for measuring open-loop characteristics.

2.3 RF Control Law

To maintain the rf gap voltage in the cavities, a software feedback program for collecting and processing data is interfaced to the hardware through the EPICS control system. The rf controllaw is an application of **sddscontrollaw** that performs simple feedback on process variables (PVs) [4]. Basically, a set of readback process variables is regulated to a set of control process variables to maintain rf gap voltage. In the present rf configuration each klystron powers a set of eight cavities in two separate rf sectors of the storage ring. There is one **sddscontrollaw** for each klystron. The hardware interface to EPICS limits the probe power reading to a 2-Hz rate.

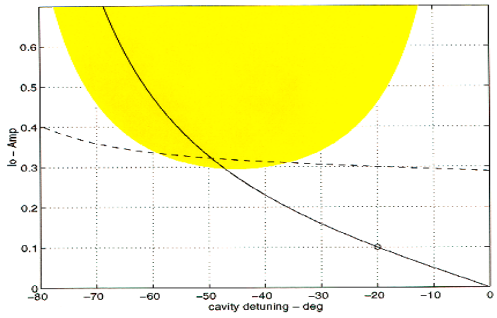

Figure 3: Bounds on beam current I_o, when cavities are detuned optimally (solid line), assuming V_{rf} = 8.0 MV.

3 BEAM DYNAMICS

3.1 Beam Loading

Computer simulation of the SR RF system for 100-mA operation with optimal detuned cavities shows that the Robinson stability criterion is satisfied, as shown in Figure 3. The Robinson stability criterion is met for the ultimate goal of 300-mA operation, with a total ring voltage of 12 MV and a cavity detuning angle of -42 degrees. For the APS storage ring cavity this amounts to a -17 kHz detuning from the no-beam resonance condition to the fully loaded condition for 300-mA beam operation. The shaded area is due to the Robinson instability, and the dashed curve is due to the available power (assumed < 3 MW) [5].

3.2 Coupled-Bunch Instability

To provide stable and useful x-rays from APS insertion devices such as undulators and wigglers, the storage ring has to supply a beam of 100 mA with a lifetime of at least 10 hours. Some coupled-bunch-related APS SR parameters are listed in Table 2.

Table 2: Some CB-related APS/SR Parameters

Beam energy	7 GeV
Maximum beam current	300 mA
Revolution frequency	271.55 kHz
Harmonic number	1296
RF frequency	351.927 MHz
Synchrotron frequency	1.8 kHz
Longitudinal damping rate	213 sec^{-1}
Cavity water temperature	75 to 95 ° F

Longitudinal coupled-bunch (CB) instability was observed in the APS storage ring. This instability was found to depend on the bunch fill pattern as well as on the beam intensity [6]. Figure 4 shows the beam spectra for a symmetric, 4x12 bunch pattern when the beam is unstable. A span of one f_{rf} is shown at a high harmonic, since the peak of the CB signals are near (bunch length)$^{-1}$. The unstable beam spectrum exhibits a coupled-bunch signature. When an interbunch phase advance corresponding to a CB mode of n=540 was introduced in the crude model using a maximum displacement of 7˚ of rf phase (55 ps), the result showed qualitative agreement with the data in Figure 4.

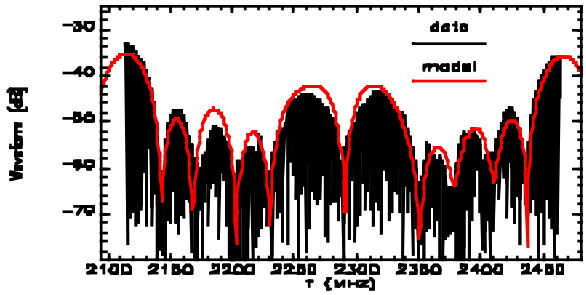

Figure 4: Unstable beam spectrum, 4x12 bunch pattern.

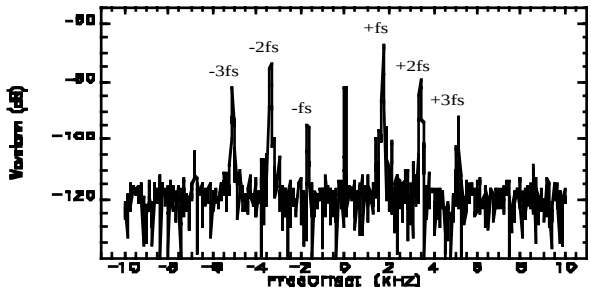

Figure 5: Unstable beam spectrum, centered at $7f_{rf}+f_{rre}$.

In a uniformly-filled ring, the CB spectrum is periodic in $f_{rf}/2$. When the fill pattern is nonuniform, the CB spectrum is highly degenerate. Synchrotron sidebands from several CB modes may be aliased onto every revolution harmonic. This is evidenced in the asymmetric

pattern of f_s sidebands in Fig. 5 for the unstable 4x12 fill pattern.

3.3 Higher-Order Modes (HOMs)

Measurements of the beam-excited rf cavity HOM spectra for different bunch patterns also suggest that the TM_{013} mode ($f \cong 1214$ MHz) is involved in the observed CB instability. The spectra were measured using E-type probes in the rf cavities. High-resolution measurements centered on a rotation harmonic revealed a large upper synchrotron sideband, excited when the beam was unstable, as shown in Figure 6 [7].

The beam fluctuations exhibited two periodicities, which were found to be correlated with the rf cavity temperatures. This intensity-dependent collective effect is driven by long-range wakefields such as those produced in the excitation by the beam of high-Q HOMs in the rf accelerating cavities. To suppress the CB instability, the cavity water supply temperatures were increased to shift HOMs out of resonance with the beam. To more effectively damp the HOMs in the storage ring rf cavities, coaxial higher-order-mode dampers with high-pass filters are being designed and tested. These are E-type and H-type probe dampers with minimal deQing at the fundamental frequency.

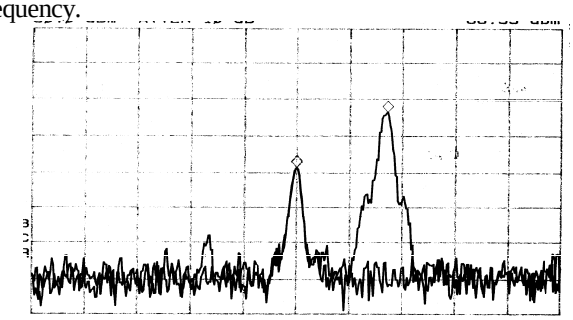

Figure6: RF cavity signal centered on a revolution harmonic at 1214.64 MHz

3.4 Beam-induced Multipactoring

Multipactoring can cause breakdown in high-power rf components like couplers, windows, etc. These phenomena can start if certain resonant conditions for electron clouds are fulfilled and if the impacted surface has a secondary yield larger than one. To protect the ceramic window of the cavity and to understand these phenomena, a newly redesigned electron detector system, initially developed at DESY, was implemented. It can extract any electron clouds that may be induced by rf, arcing, or even x-rays from the upstream bending magnet.

Preliminary data was taken recently after a bad input coupler was replaced with a refurbished one in the sector 36 #2 cavity, as shown in Figure 7. The green line (step-like pulse) is from the #2 cavity, compared to the blue line from the #1 cavity. While there is no activity in any other cavities, the pulsed signal from the #2 cavity repeats at about 80 seconds with the width of 20 seconds. This signal is about 3.5 V, which corresponds to 3.5 μA. The pulse width appears to be longer and higher with the higher stored beam current and/or rf power in the cavity.

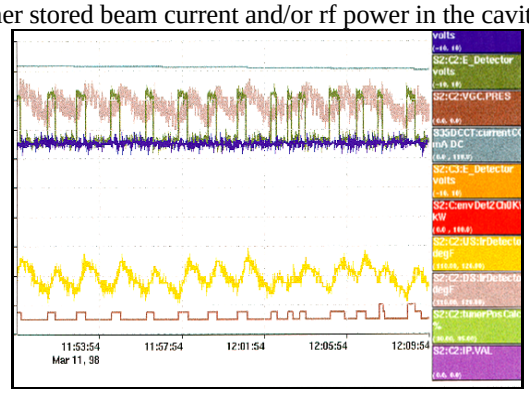

Figure 7: Electron cloud signal from the newly replaced ceramic window; also shown are vacuum pressure and ceramic temperature from the infrared cameras.

Also shown is the vacuum pressure in the cavity (gray step-like pulse at the bottom). The pressure changes are very small, but they are consistent with the electron clouds, which indicates outgassing in the cavity locally. The ceramic temperature, which was taken from the upstream and downstream ceramic window with the infrared cameras, also follows whenever the electron is induced in the cavity (two curves: yellow and light-gray).

The input coupler in that cavity had been replaced three times within last two years. The ceramic windows were vacuum-leaked and deposited with copper, and the damaged area appeared to match the x-ray trajectory from the upstream bending magnet. Since there apparently was insufficient shielding, the x-rays from the upstream bending magnet had directly penetrated the Aluminum waveguide and hit the #2 cavity input coupler/ceramic window. More shielding was added, and a detailed analysis will be done when more data and simulation results are available.

4 REFERENCES

[1] A. Nassiri et al., "An Overview of the APS 352-MHz RF Systems," Proc. of the 1997 Particle Accelerator Conference, Vancouver, Canada, to be published.

[2] Y.W. Kang et al., "Reconfigurable High-Power RF System in the APS," Proc. of the 1997 Particle Accelerator Conference, Vancouver, Canada, to be published.

[3] D. Horan et al., "Phase Loop Bandwidth Measurements on the Advanced Photon Source 352-MHz RF Systems," Proc. of the 1997 Particle Accelerator Conference, Vancouver, Canada, to be published.

[4] L. Emery, "Commissioning Software Tools at the Advanced Photon Source," Proc. of the 1995 Particle Accelerator Conference, p. 2238 (1996).

[5] C. Schwartz et al., "Simulation of the APS Storage-Ring RF Accelerating System," Proc. of the 1997 Particle Accelerator Conference, Vancouver, Canada, to be published.

[6] K. Harkay et al., "Compensation of Longitudinal Coupled-Bunch Instability in the Advanced Photon Source Storage Ring," Proc. of the 1997 Particle Accelerator Conference, Vancouver, Canada, to be published.

[7] J.J. Song et al., "Higher-Order Modes of the Storage Ring RF Cavities," Proc. of the 1997 Particle Accelerator Conference, Vancouver, Canada, to be published.